

Photoemission and inverse-photoemission study of superconducting $\text{YNi}_2\text{B}_2\text{C}$: Effects of electron-electron and electron-phonon interactions

A. Fujimori, K. Kobayashi, T. Mizokawa, K. Mamiya, and A. Sekiyama
Department of Physics, University of Tokyo, Bunkyo-ku, Tokyo 113, Japan

H. Eisaki, H. Takagi,* and S. Uchida
Department of Applied Physics, University of Tokyo, Bunkyo-ku, Tokyo 113, Japan

R. J. Cava, J. J. Krajewski, and W. F. Peck, Jr.
AT&T Bell Laboratories, Murray Hill, New Jersey 07974
(Received 13 May 1994; revised manuscript received 27 June 1994)

We have studied the electronic structure of the superconductor $\text{YNi}_2\text{B}_2\text{C}$ by photoemission and inverse-photoemission spectroscopy. The spectra show a prominent Ni $3d$ band centered around 1.5 eV below the Fermi level (E_F), whose top crosses E_F , and B, C $2sp$ -derived states at higher binding energies, generally consistent with band-structure calculations. However, the Ni $3d$ -derived conduction bands are narrower than calculated and are accompanied by a satellite, signaling electron-correlation effects within the d bands. The density-of-states peak at E_F predicted by band-structure calculations is suppressed and its spectral weight is transferred away from E_F , presumably due to an electron-phonon interaction and/or electron correlation.

The discovery of superconductivity in boride-carbide systems, Y-Pd-B-C ($T_c = 23.2$ K) (Ref. 1), $\text{RNi}_2\text{B}_2\text{C}$ ($R = \text{Y, Lu, Tm, Er, and Ho}$, $T_c = 16.6$ K for $R = \text{Lu}$) (Ref. 2), and Y-Ni-B-C ($T_c \sim 13$ K) (Ref. 3) has invoked renewed interest in the search for high-temperature superconductivity in multinary intermetallics. Each family of superconductors so far discovered, including A15 compounds, Chevrel-phase compounds, cuprates, and fullerides, possesses characteristic structural and electronic features, which have been thought to be related to the appearance of superconductivity. The electronic structure of transition-metal borides and carbides has generally been characterized by strong covalent bonding between the constituent elements.⁴ The layered structure of $\text{RNi}_2\text{B}_2\text{C}$, which consists of alternating stacks of RC and Ni_2B_2 units,⁵ and the presence of the late transition element Ni suggests some analogy with the cuprate superconductors. The extent to which electron correlation and two-dimensionality play roles in the Ni boride carbides is therefore of primary interest and has to be clarified experimentally. Mattheiss⁶ has performed band-structure calculations on $\text{RNi}_2\text{B}_2\text{C}$ using the local-density approximation (LDA), and has shown that the energy bands which cross the Fermi level (E_F) are dominated by Ni $3d$ character. Most remarkably, the calculated density of states (DOS) shows a peak at E_F , arising from a relatively dispersionless energy band which is located close to E_F . Photoemission spectroscopy is well suited to study energy-band structures, electron correlation, and other interaction effects. In this paper, we report on our photoemission and inverse-photoemission studies of $\text{YNi}_2\text{B}_2\text{C}$. We have chosen $R = \text{Y}$ ($T_c = 15.6$ K) because the presence of rare-earth $4f$ states would obscure spectral features from other valence- and conduction-band states which are relevant to the superconductivity.

Polycrystalline samples of $\text{YNi}_2\text{B}_2\text{C}$ were prepared by arc melting and subsequent annealing. Details of the sample

preparation are given in Ref. 2. Photoemission experiments were performed at beamline BL-2 of the Synchrotron Radiation Laboratory, Institute for Solid State Physics, University of Tokyo. The total instrumental resolution varied from ~ 0.3 eV at $h\nu \sim 40$ eV to ~ 0.6 eV at $h\nu \sim 100$ eV, determined by the width of the Fermi edge of evaporated Au. The position of the Au Fermi edge has been used to calibrate the binding energies. Measurements were also made on a spectrometer equipped with a He discharge lamp ($h\nu = 21.2$ eV) with a resolution of ~ 0.1 eV. Inverse-photoemission spectroscopy or bremsstrahlung-isochromat spectroscopy (BIS) measurements were made at $h\nu = 1486.6$ eV using a quartz monochromator. The E_F position and the energy resolution (~ 1 eV) were determined by measuring the Fermi edge of Au evaporated on the sample. The samples were cooled to liquid-nitrogen temperature and scraped *in situ* with a diamond file. The base pressures in the spectrometers were $1-2 \times 10^{-10}$ Torr.

Figure 1 shows photoemission spectra measured using synchrotron radiation. The photoionization cross section of the Ni $3d$ orbitals relative to the B and C $2sp$ orbitals rapidly increases with increasing photon energy⁷ (except for the Ni $3p \rightarrow 3d$ resonance at $h\nu \sim 65-70$ eV discussed below). Therefore, from comparison between the $h\nu = 63$ eV and $h\nu = 100$ eV spectra, one can conclude that the prominent emission centered at ~ 1.5 eV below E_F is largely due to Ni $3d$, and that the structures at ~ 6 , ~ 10 , and ~ 14 eV have significant B and/or C $2sp$ character, confirming the result of the band-structure calculations.^{6,8} In accordance with the calculations, the BIS spectrum shown in Fig. 2 shows the unoccupied part of the Ni $3d$ -derived conduction bands extending from E_F to ~ 1.5 eV above it, and the almost empty Y $4d$ band centered at ~ 6 eV above E_F . Thus the Fermi level is located in the upper part of the Ni $3d$ -derived conduction bands and results in the sharp Fermi cutoff both in the photoemission and BIS spectra.

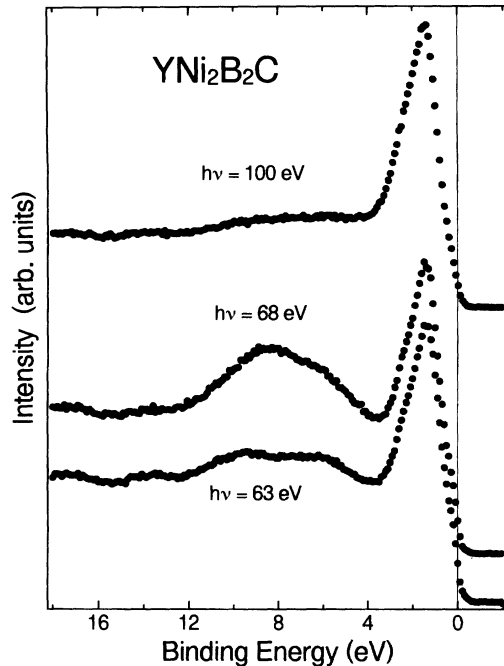


FIG. 1. Photoemission spectra of $\text{YNi}_2\text{B}_2\text{C}$.

In order to see to what extent the calculated band structure is appropriate, or to what extent electron-electron and other interaction effects neglected in the band-structure calculations are important in describing the electronic properties of $\text{YNi}_2\text{B}_2\text{C}$, we have made detailed comparison between the measured spectra and the band-structure calculations⁶ as shown in Figs. 3 and 4. To obtain the theoretical spectra from the band-structure calculations, the partial DOS of each atomic-orbital component has been weighted by the corresponding atomic-orbital photoionization cross section.⁷ The instrumental resolution and the lifetime broadening have been taken into account through convolution of the DOS with Gaussian and Lorentzian functions, respectively;⁹ integral backgrounds have also been superimposed. The calculated and measured photoemission spectra are approximately normalized to the integrated intensities. In Fig. 3, the photo-

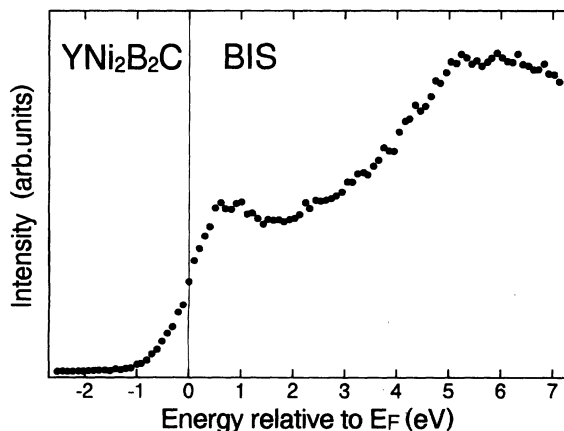


FIG. 2. BIS spectrum of $\text{YNi}_2\text{B}_2\text{C}$.

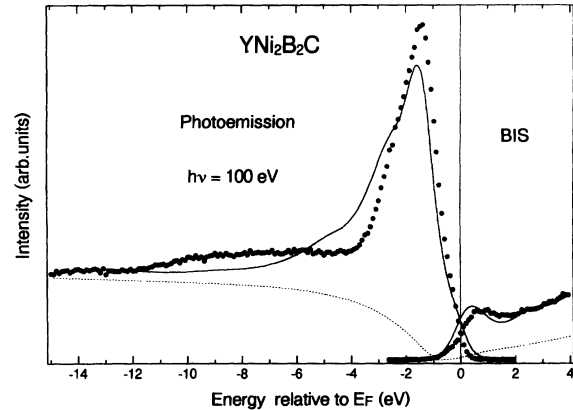


FIG. 3. Comparison of the photoemission and BIS spectra (dots) with the band-structure calculations by Mattheiss (Ref. 6) (solid lines). The theoretical curves have been synthesized and normalized as described in the text.

emission and BIS spectra have been scaled so that their intensities coincide at E_F .

The Ni 3d emission centered at ~ 1.5 eV is shifted towards E_F by ~ 0.2 eV compared to the LDA band-structure calculations, whereas the B- and C-hybridized features at ~ 6 , ~ 10 , and ~ 14 eV are all shifted away from E_F by ~ 1 eV (e.g., the observed ~ 6 eV corresponds to the calculated shoulder at ~ 5 eV). In Fig. 3, the most remarkable discrepancy between theory and experiment is that the observed width of the Ni 3d band is reduced by $\sim 20\%$ as a whole compared to the calculations. Furthermore, the measured spectra show extra spectral weight at 5–10 eV below E_F . Since at $h\nu = 100$ eV, the photoionization cross sections for the B and C orbitals are negligibly small compared to that of Ni 3d, the extra spectral weight is attributed to a Ni 3d origin. It is well known that in Ni metal, the Ni 3d bands are

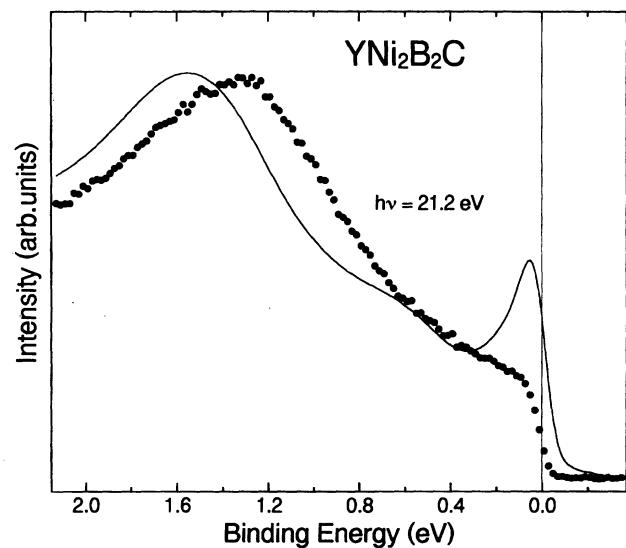


FIG. 4. Comparison of the photoemission spectrum near E_F (dots) with the band-structure calculations by Mattheiss (Ref. 6) (solid lines). The same as Fig. 3. The spectra have been normalized to the peak intensities.

narrowed by $\sim 30\%$ compared to LDA band-structure calculations, and that a satellite appears at 6 eV below E_F due to electron correlation within the d bands.¹⁰ The present result therefore indicates that electron correlation is significant in $\text{YNi}_2\text{B}_2\text{C}$ (although it is paramagnetic while Ni metal is ferromagnetic). The satellite in Ni metal has been attributed to a two-hole bound state and is enhanced for photon energies in the Ni $3p \rightarrow 3d$ core-excitation region via resonance-photoemission effects. Indeed, the $h\nu = 68$ eV spectrum in Fig. 1 shows an enhancement around ~ 8 eV below E_F . This satellite position is deeper than that in Ni metal, shallower than in NiO (~ 10 eV below E_F),¹¹ and nearly the same as in NiS,¹² suggesting that the d - d Coulomb energy U is intermediate between that in Ni metal ($U \sim 2$ eV) (Ref. 10) and that in NiO ($U \sim 7$ – 8 eV) (Ref. 13), and is similar to that in NiS ($U \sim 4$ eV) (Ref. 12). A crude estimate using the binding energy of the satellite, $E_B(d^8) \sim 8$ eV, and that of the Ni $3d$ band, $E_B(\text{Ni } 3d) \sim 1.5$ eV, also leads to a similar value: $U \sim E_B(d^8) - 2E_B(\text{Ni } 3d) \sim 5$ eV. The U value of $\text{YNi}_2\text{B}_2\text{C}$ indicates that the screening of the Coulomb interaction is more efficient than in NiO, which is highly insulating, while it is less efficient than in Ni metal (and its alloys), where d - d Coulomb interaction is screened by $4s$ conduction electrons. As for the discrepancy between experiment and theory for the energy positions of the B- and C-derived features, similar discrepancies have been found for sp states in other transition-metal compounds¹⁴ and would also be attributed to a limitation of the LDA calculations.

In addition to the band narrowing and the satellite formation mentioned above, spectral features in the vicinity of E_F show further discrepancy between theory and experiment: as can be seen from the high-resolution spectrum in Fig. 4, the band-structure calculations predict a remarkable DOS peak at E_F whereas the measured spectra show a Fermi cutoff without any sign of such a peak. This behavior is also evident in the BIS spectrum, if we take into account the lower energy resolution of BIS: the Fermi-level position in the calculated spectrum is located closer to the peak while the measured Fermi-level position lies in the middle of the leading edge as would be expected for a flat DOS. The discrepancy between experiment and theory for the $h\nu = 100$ eV spectrum, whose resolution is also low, is consistent with this interpretation. When the DOS peak at E_F is suppressed in the photoemission spectra, the lost spectral weight must be redistributed away from E_F . The comparison between the experimental and theoretical BIS spectra in Fig. 3 indeed implies a spectral weight transfer from near E_F to ~ 0.5 – 1 eV above it within the limited experimental resolution. The measured and calculated photoemission spectra in the same figure, which are normalized to the integrated intensities, also imply a spectral weight transfer from E_F towards 0.5 – 1 eV below E_F , although it is not so obvious as in the BIS spectra due to the overlap of the strong Ni d -band peak centered ~ 1.5 eV below E_F .

The suppression of the DOS peak at E_F and the associated spectral weight transfer on the energy scale of 0.5 – 1 eV may be reminiscent of a pseudogap formation in the DOS on that energy scale, as has been predicted for strongly coupled electron-phonon systems^{15,16} and electrons interacting with spin fluctuations.¹⁷ From comparison between the measured and calculated photoemission spectra (Fig. 4), the DOS at

E_F is suppressed by a factor of ~ 0.5 . Nevertheless, the quasiparticle DOS at E_F derived from the electronic specific heat jump at T_c (~ 25 mJ/mol K²) (Ref. 18) is larger than the DOS given by the band-structure calculations (4.8 states/mol eV) (Ref. 6) by a factor of ~ 2 , which is even larger than the inverse of the overall band narrowing factor ~ 1.2 for the Ni $3d$ bands, indicating that the band narrowing becomes more pronounced as the Fermi level is approached.¹⁹ The mass enhancement or band narrowing on the low energy scale should generally be accompanied by a reduction of the quasiparticle spectral weight near E_F ; the lost spectral weight should be redistributed away from E_F as incoherent spectral weight on that energy scale. The origin of the mass enhancement on the low energy scale may be due to electron correlation (including spin fluctuation effects), which is generally energy dependent, and/or electron-phonon interaction, which is effective only at low energies. If one considers high-frequency optical phonons due to vibrations of light B and C atoms and assumes a strong electron-phonon coupling, the energy scale of 0.5 – 1 eV may be realized.

Finally, we note that the appearance of a DOS peak arising from a flat band near E_F in band-structure calculations, and its intensity suppression in photoemission spectra, is a rather common feature of various high- T_c superconductors, although the underlying band structures are quite different between the different materials⁶ (i.e., wide nondegenerate p - $d\sigma^*$ or s - $p\sigma^*$ antibonding bands for cuprates and Bi oxides and narrow d bands for the present boride carbides, A15 compounds, and Chevrel-phase compounds). For $\text{BaPb}_{1-x}\text{Bi}_x\text{O}_3$ and $\text{Ba}_{1-x}\text{K}_x\text{BiO}_3$, band-structure calculations predict a DOS peak at or close to E_F (Ref. 20) whereas measured spectra exhibit an intensity decrease towards E_F .²¹ In A15 compounds, a predicted sharp DOS peak close to E_F was not observed in a high-resolution photoemission study²² while the quasiparticle peak of a flat band, although considerably broadened, has been identified by angle-resolved photoemission spectroscopy,²³ suggesting a considerable transfer of the quasiparticle spectral weight towards high energies. In $\text{Bi}_2\text{Sr}_2\text{CaCu}_2\text{O}_{8+\delta}$, band-structure calculations have predicted a DOS peak ~ 0.5 eV below E_F arising from flat bands;²⁴ according to an angle-resolved photoemission study, such bands are located very close to E_F (\sim within 0.05 eV) (Ref. 25) but have not been identified as a peak in angle-integrated photoemission spectra.²⁶

In conclusion, the gross electronic structure of $\text{YNi}_2\text{B}_2\text{C}$ is well described by the LDA band-structure calculations, while electron correlation manifests itself as a moderate narrowing of the Ni $3d$ -derived conduction bands and the appearance of a two-hole bound-state satellite. Energy bands in the vicinity of E_F are further narrowed due to coupling with low-energy excitations, such as phonons and spin fluctuations, and at the same time the DOS peak at E_F is suppressed. More detailed information is clearly needed to characterize the electronic states in the vicinity of E_F , e.g., by angle-resolved photoemission. Comparison with Y-Pd-B-C will also shed more light on the electronic structure and superconductivity in the boride-carbide systems.

The results of the band-structure calculations were kindly

provided by L. F. Mattheiss prior to publication. We would like to thank the staff of the Synchrotron Radiation Laboratory for valuable technical support. The work at the Univer-

sity of Tokyo is supported by Grants-in-Aid for Scientific Research from the Ministry of Education, Science and Culture of Japan.

[†]Present address: Institute for Solid State Physics, University of Tokyo, Roppongi, Tokyo 106, Japan.

- ¹R. J. Cava, H. Takagi, B. Batlogg, H. W. Zandbergen, J. J. Krajewski, W. F. Peck, Jr., R. B. van Dover, R. J. Felder, T. Siegrisy, K. Mizuhashi, J. O. Lee, H. Eisaki, S. A. Carter, and S. Uchida, *Nature* **367**, 146 (1994).
- ²R. J. Cava, H. Takagi, H. W. Zandbergen, J. J. Krajewski, W. F. Peck, Jr., T. Siegrisy, B. Batlogg, R. B. Van Dover, R. J. Felder, K. Mizuhashi, J. O. Lee, H. Eisaki, and S. Uchida, *Nature* **367**, 252 (1994); H. Takagi, R. J. Cava, H. Eisaki, J. O. Lee, K. Mizuhashi, B. Batlogg, S. Uchida, J. J. Krajewski, and W. F. Peck, Jr., *Physica C* (to be published).
- ³R. Nagarajan, C. Mazumdar, Z. Hossain, S. K. Dhar, K. V. Gopalakrishnan, L. C. Gupta, C. Godart, B. D. Padalia, and R. Vijayaraghavan, *Phys. Rev. Lett.* **72**, 274 (1994).
- ⁴See, e.g., A. Neckel, P. Rastl, R. Eibler, P. Weinberger, and K. Schwarz, *J. Phys. C* **9**, 579 (1976).
- ⁵T. Siegrist, H. W. Zandbergen, R. J. Cava, J. J. Krajewski, and W. F. Peck, Jr., *Nature* **367**, 254 (1994).
- ⁶L. F. Mattheiss, *Phys. Rev. B* **49**, 13 279 (1994).
- ⁷According to Hartree-Fock-Slater atomic calculations [J.-J. Yeh and I. Lindau, *At. Data Nucl. Data Tables* **32**, 1 (1985)], $\sigma(\text{B } 2sp)/\sigma(\text{Ni } 3d) \sim 3, 0.2, \text{ and } 0.1$, $\sigma(\text{C } 2sp)/\sigma(\text{Ni } 3d) \sim 5, 0.2, \text{ and } 0.1$ and $\sigma(\text{Y } 4d)/\sigma(\text{Ni } 3d) \sim 10, 0.03, \text{ and } 0.03$ for $h\nu = 21.2, 60, \text{ and } 100$ eV, respectively, where $\sigma(M nl)$ denotes the photoionization of cross section of the $M nl$ orbital per electron. For BIS ($h\nu = 1486.6$ eV), $\sigma(\text{C } 2p)/\sigma(\text{Ni } 3d) \sim 0.007$ and $\sigma(\text{Y } 4d)/\sigma(\text{Ni } 3d) \sim 0.6$.
- ⁸The structure at ~ 10 eV below E_F may partly be due to contamination (probably from grain boundaries of the polycrystalline sample) because its intensity for low photon energies became too large compared to the structures at ~ 6 and ~ 14 eV, incompatible with the band-structure calculations.
- ⁹The lifetime increases as one moves away from E_F : we have assumed that $\text{FWHM} = \alpha|E - E_F|$, where α is chosen 0.3 below E_F and 0.2 above E_F .
- ¹⁰D. R. Penn, *Phys. Rev. Lett.* **42**, 921 (1979); L. C. Davis and L. A. Feldkamp, *Solid State Commun.* **34**, 141 (1980).
- ¹¹G. A. Sawatzky and J. W. Allen, *Phys. Rev. Lett.* **53**, 2339 (1984).
- ¹²A. Fujimori, K. Terakura, M. Taniguchi, S. Ogawa, S. Suga, M. Matoba, and S. Anzai, *Phys. Rev. B* **37**, 3109 (1988).
- ¹³A. Fujimori and F. Minami, *Phys. Rev. B* **30**, 957 (1984).
- ¹⁴See, e.g., J. H. Weaver, A. M. Bradshaw, J. F. van der Veen, F. J. Himpsel, D. E. Eastman, and C. Politis, *Phys. Rev. B* **22**, 4921 (1980).
- ¹⁵K.-M. Ho, M. L. Cohen, and W. E. Pickett, *Phys. Rev. Lett.* **41**, 815 (1978).
- ¹⁶M. Vekic and S. R. White, *Phys. Rev. B* **48**, 7643 (1993).
- ¹⁷A. Kampf and J. R. Schieffer, *Phys. Rev. B* **41**, 6339 (1990).
- ¹⁸S. A. Carter *et al.* (unpublished); H. Takagi (unpublished).
- ¹⁹We may factorize the mass enhancement of ~ 2 on the low-energy scale into the negative contribution from the k dependence of the self-energy, ~ 0.5 , which suppresses the DOS and the photoemission intensity at E_F , and the positive contribution from the energy dependence of the self-energy, $\sim 2/0.5 = 4$, which increases the quasiparticle DOS at E_F but conserves the photoemission intensity at E_F . See, e.g., C. W. Greeff, H. R. Glyde, and B. E. Clements, *Phys. Rev. B* **45**, 7951 (1992).
- ²⁰L. F. Mattheiss and D. R. Hamann, *Phys. Rev. B* **28**, 4227 (1983).
- ²¹H. Namatame, A. Fujimori, H. Takagi, S. Uchida, F. M. F. de Groot, and J. C. Fuggle, *Phys. Rev. B* **48**, 15 917 (1993); H. Namatame, A. Fujimori, H. Torii, N. Suzuki, T. Uchida, Y. Nagata, and J. Akimitsu, *Phys. Rev. B* (to be published).
- ²²M. Grioni, D. Malterre, B. Dardel, J.-M. Imer, Y. Baer, J. Muller, J. L. Jorda, and Y. Petroff, *Phys. Rev. B* **43**, 1216 (1991).
- ²³M. Aono, F. J. Himpsel, and D. E. Eastman, *Solid State Commun.* **39**, 225 (1981).
- ²⁴S. Massida, J. J. Yu, and A. J. Freeman, *Physica C* **152**, 251 (1988).
- ²⁵D. S. Dessau, Z.-X. Shen, D. M. King, D. S. Marshall, L. W. Lombardo, P. H. Dickinson, J. DiCarlo, C.-H. Park, A. G. Loeser, A. Kapitulnik, and W. E. Spicer, *Phys. Rev. Lett.* **71**, 2781 (1993).
- ²⁶J.-M. Imer, F. Patthey, B. Dardel, W.-D. Schneider, Y. Baer, Y. Petroff, and A. Zettl, *Phys. Rev. Lett.* **62**, 336 (1989).